

Lab on a Chip

Accepted Manuscript



This is an *Accepted Manuscript*, which has been through the Royal Society of Chemistry peer review process and has been accepted for publication.

Accepted Manuscripts are published online shortly after acceptance, before technical editing, formatting and proof reading. Using this free service, authors can make their results available to the community, in citable form, before we publish the edited article. We will replace this *Accepted Manuscript* with the edited and formatted *Advance Article* as soon as it is available.

You can find more information about *Accepted Manuscripts* in the [Information for Authors](#).

Please note that technical editing may introduce minor changes to the text and/or graphics, which may alter content. The journal's standard [Terms & Conditions](#) and the [Ethical guidelines](#) still apply. In no event shall the Royal Society of Chemistry be held responsible for any errors or omissions in this *Accepted Manuscript* or any consequences arising from the use of any information it contains.

ARTICLE

Magnetic micro-device for manipulating PC12 cells migration and organization

Cite this: DOI: 10.1039/x0xx00000x

N. Alon^{a,d}, T. Havdala^{b,d}, H. Skaat^{c,d}, K. Baranes^{a,d}, M. Marcus^{a,d}, I. Levy^{c,d}, S. Margel^{c,d}, A. Sharoni^{b,d,†} and O. Shefi^{a,d,†}Received 00th January 2015,
Accepted 00th January 2015

DOI: 10.1039/x0xx00000x

www.rsc.org/

Directing neuronal migration and growth has an important impact on potential therapies post trauma. Using magnetic manipulations is an advantageous method for guiding remotely cells. In the present study we have generated highly localized magnetic fields with controllable magnetic flux densities to manipulate neuron-like cells migration and organization at the micro-scale level. We designed and fabricated a unique miniaturized magnetic device, an array of rectangular ferromagnetic bars made of permalloy (Ni₈₀Fe₂₀), sputter-deposited onto glass substrates. The asymmetric shape of the magnets enables to design a magnetic landscape with high flux densities at the poles. Iron oxide nanoparticles were introduced into PC12 cells, making the cells magnetically sensitive. First, we manipulated the cells by applying an external magnetic field. The magnetic force was strong enough to direct PC12 cells migration in culture. Based on time lapse observations, we analysed the cells' movement and estimated the amount of MNPs per cell. We plated the uploaded cells on the micro-patterned magnetic device. The cells migrated towards the high magnetic flux zones and aggregated at the edges of the patterned magnets, corroborating that the cells with magnetic nanoparticles are indeed affected by the micro-magnets and attracted to the bars' magnetic poles. Our study presents an emerging method for the generation of pre-programmed magnetic micro- 'hot spots' to locate and direct cellular growth, setting the stage for implanted magnetic device.

Introduction

Recent advances in nanotechnology pose magnetic manipulations as a promising method for guiding remotely neuronal motility and growth, with important implications in research and potential therapeutics. Physical forces play a key role in shaping neuronal structure. Specifically, cellular mechanical tension is a major effector in the development and morphogenesis of neurons and neural networks formation¹⁻⁵. It has been demonstrated that mechanical pulling of neuronal processes has the ability to modify processes fate and role within the cell^{6,7}. In previous studies magnetic forces have been used to apply tensile forces on neurons and mechanically pull neurites along growth. Odde and colleagues have attached magnetic micro-beads to neuronal membranes and pulled the beads using an external electromagnet. The neuronal membrane was stretched, and an axon was initiated and elongated^{8,9}.

Magnetic particles at the nano-scale can also mediate magnetic manipulations if a sufficient amount is incorporated into the cells. Iron oxide nanoparticles (Fe₂O₃ or Fe₃O₄) have the necessary magnetic properties and have previously been used for positioning non-neuronal cells in response to an external magnetic field¹⁰⁻¹². Conditioning PC12 cells with high

concentration of iron oxide nanoparticles, in addition to the regular differentiation treatment with a nerve growth factor (NGF), has led to enhanced cellular sprouting with no cytotoxic effects, even without applying magnetic field¹³. We have shown that using iron oxide nanoparticles conjugated to NGF enhanced NGF stability and promoted PC12 cells differentiation and growth¹⁴. In a subsequent study Riggio et al. also used magnetic iron oxide nanoparticles carrying NGF and applied an external magnetic field. The nanoparticles induced neurite sprouting with growth preferentially directed according to the magnetic force¹⁵. Recent studies have attempted to apply magnetic fields locally in order to affect selected sets of cells. Lee et al., have developed micro electromagnetic matrix to manipulate cells^{16,17}. Tseng et al. have fabricated round symmetric magnetic pads embedded in the culture substrate. An external magnetic field was applied and the pads that served as attractive spots, affected the cellular migration¹⁸.

In the present study we designed and generated magnetic fields with controllable magnetic flux densities, at multiple scales of size and strength. We uploaded PC12 cells with iron oxide nanoparticles and analyzed their migration and growth pattern. First, we applied an external magnetic field. We analyzed the dynamic of movement of the PC12 cells and

extracted the effective magnetic force. This allowed us to estimate the amount of magnetic nanoparticles that single cells uptake. Then, we designed and fabricated a unique device, a substrate embedded with micropatterned ferromagnets that can be magnetized selectively. The asymmetric shape of the patterned magnets enabled to 'build' a significant magnetic field with high flux densities at the edges (poles) of the micro-magnets or alternatively to 'break' the directed magnetization into domains with no net magnetic field. The PC12 cells that were uploaded with the iron oxide magnetic nanoparticles migrated toward the high magnetic flux zones, demonstrating the formation of an organized aggregation.

Our study presents an emerging method for miniaturizing a magnetic-based device embedded with magnetic 'hot spots' to locate and direct neuron-like cells. Such development is opening new directions in non-invasive control of cells remotely.

Results and discussion

Synthesis, characterization and cellular uptake of iron oxide nanoparticles

We used fluorescent magnetic nanoparticles (MNPs), maghemite, $\gamma\text{-Fe}_2\text{O}_3$, as mediators to apply physical forces on the cells. The nanoparticles were synthesized by nucleation, followed by controlled growth of $\gamma\text{-Fe}_2\text{O}_3$ thin films onto gelatin-RITC-iron oxide nuclei (RITC i.e. Rhodamine Isothiocyanate). In order to achieve a strong magnetization per nanoparticle, six layers were synthesized (for details see

Experimental section). PC12 cells were incubated in medium enriched with the iron oxide nanoparticles, prior to plating. The cells demonstrated an uptake of the nanoparticles, with no cytotoxic effect (Figs. 1(A,B)). Cells viability following the incubation with the MNPs was examined using an XTT assay. 99% of the PC12 cells were found viable after 5 days of incubation, normalized to cells with no MNPs (Fig. 1(B)). It can be seen that the cells became fluorescent with a dark shadow in the center reflecting the nuclei location. Fluorescent confocal images of the cells in higher magnification verify the internalization of the MNPs into the cells (Fig. 1(C)).

External magnetic field for triggering cell migration and for measuring cell magnetization

Following the incubation of PC12 cells in the magnetic nanoparticles enriched medium, cells were plated in culture (see Experimental section). Then, a magnetic field was induced by an external permanent magnet that was placed at one side of the culture dish. Time lapse observations demonstrated a movement of the cells towards the external magnet. Fig. 2(A) demonstrates the position of one single cell along 3.5min, moving from left to right. At some point, after 2.5min, an additional magnetized cell entered the frame (left side). From these measurements we can calculate the velocity and direction of motion of the cells. We confirmed that the motion is due to the permanent magnet, evidenced in Fig. 2(B) where the blue arrows indicate the motion direction of each cell. Placing the permanent magnet close to one side of the

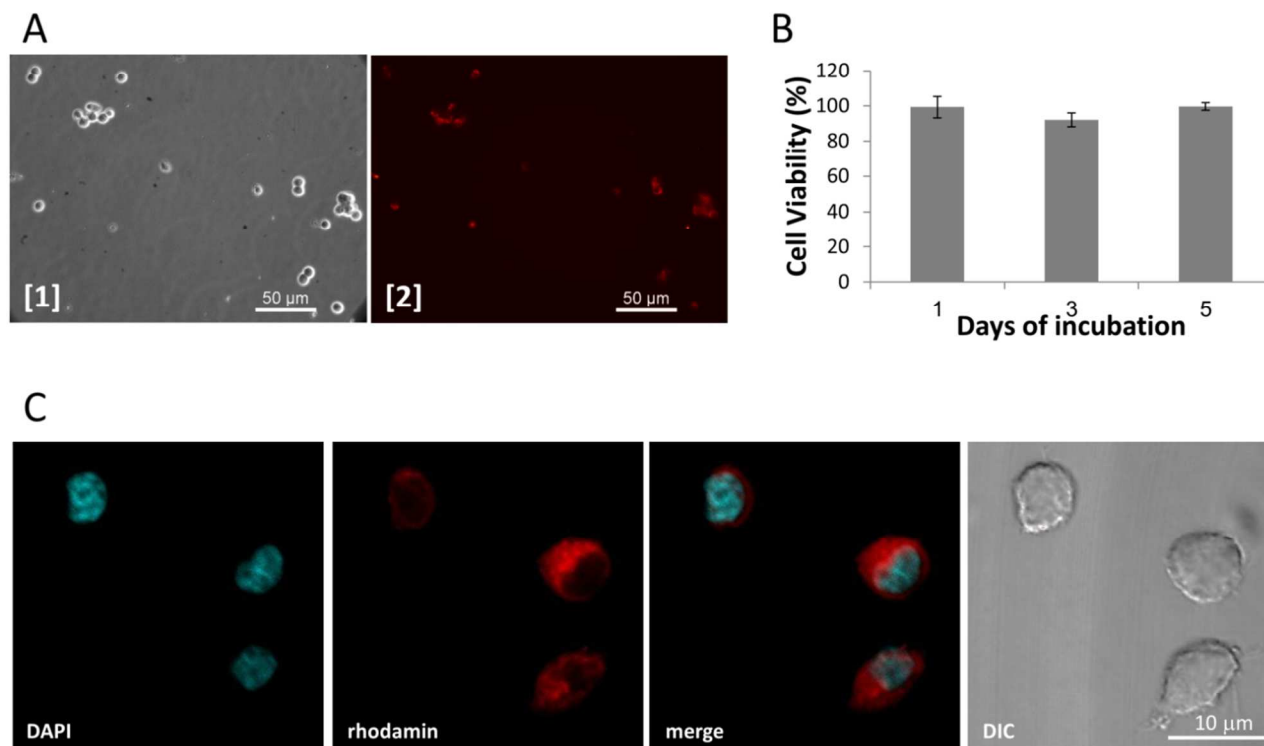


Fig. 1 (A) Uptake of MNPs by PC12 cells. (1) Phase contrast image and (2) fluorescent image of the cells after 24 h incubation with the fluorescent MNPs. (B) XTT cell viability assay. The cell viability was calculated as the percentage of surviving cells, compared to control, after 24 h and 72 h and 5 days of incubation with MNPs. (C) Confocal microscopy images of PC12 cells after 24h incubation with the fluorescent MNPs. MNPs labelled with rhodamin (red) enter the cells. Nuclei marked with DAPI (blue). The fluorescent images were acquired at a single focal plane. Upper left image: DIC image of the same labelled cells.

ARTICLE

culture led to a movement towards the magnet (Fig. 2(B)i). Changing the side of the magnet changed the direction of movement accordingly, towards the magnet in its new location (Fig. 2(B)ii). As a control, cells treated with MNPs with no external magnetic field were followed for the same period of time. Fig. S2 presents the location of representing cells along the 3.5 min. It can be seen that the direction of movement of each cell is arbitrary with much shorter distances of movement.

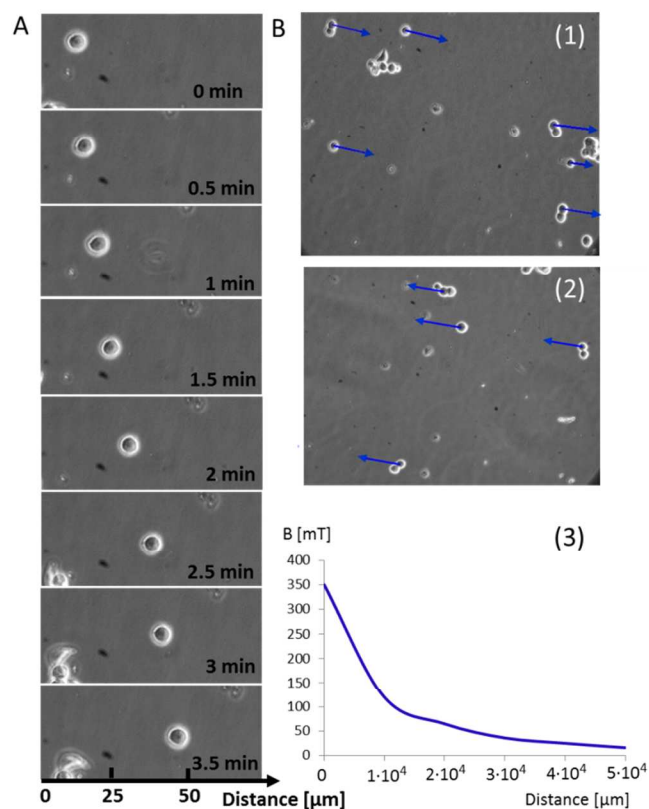


Fig. 2 (A) Time-lapse images of a cell treated with MNPs and directed to the right by a permanent magnet, which induces an external magnetic field of ~ 50 mT. (B) The velocity vectors of PC12 cells were calculated and are represented as blue arrows. (1) Velocity vectors in the presence of an external magnetic field of ~ 50 mT. (2) Velocity vectors under the same magnetic field in the opposite direction. (3) A plot describing the magnetic field gradient induced by the permanent magnet, according to measurements.

The average velocity of the cells was measured, based on the cells' velocity vectors, $v = 10.4 \pm 1.2 \mu\text{m}/\text{min}$. Fig. 2(B)iii presents the measured magnetic field as a function of distance from the magnet. The velocity was measured for cells at the center of the culture dish, where the magnetic field was about 50 mT. It is important to note that since the MNP has a

magnetic dipole, the magnetic force that triggers the movement of the magnetized cells is proportional to the gradient of magnetic field and not the absolute magnetic field. The constant velocity measured for the cells indicates that the magnetic force ($\mathbf{F}_{\text{mag}} = \mathbf{V}_x \cdot \mathbf{M}_{\text{sat}} \cdot \mu_0^{-1} \cdot \nabla \mathbf{B}_x$) is balanced by the cell drag force ($\mathbf{F}_{\text{drag}} = 3\pi \cdot \mu \cdot \mathbf{d}_{\text{cell}} \cdot \mathbf{v}$). Using the field gradient from Fig. 2(B)iii, the cell velocity and solution viscosity we calculate the effective magnetization of the cells. Next, from the MNP average volume and magnetization properties we can extract the volume and number of MNPs clustered per cell. The number of magnetic nanoparticles that were incorporated into the cells following incubation is approximately 10,000 MNPs per cell (for detailed calculation see supplementary material).

Designing and fabricating a micropatterned magnetic device for local magnetic manipulations

A miniaturized device of a substrate patterned with micron size bar-magnets was designed and fabricated to control cell migration and network formation locally. An array of bar-magnets, made of ferromagnetic permalloy ($\text{Ni}_{80}\text{Fe}_{20}$), were sputter-deposited onto glass substrates via standard liftoff-photolithography. The bars were designed as long rectangles, 300 μm long, 50 μm wide and 100nm thick (see Fig. 3). The entire device was coated with a thin layer of insulating Al_2O_3 to prevent possible effects from the metallic nature of the permalloy. Fig. 4 presents simulation results of the magnetic field as generated by a single pad, a micron above the device (for details see experimental section). It can be seen that the unique shape and dimensions of the magnetic pads lead to a magnetic field up to 350 mT and a large magnetic gradient above the edges of the rectangles. Fig. 5 indicates the size and direction of the magnetic field above the edges, demonstrating two 'hot spots' that will attract magnetic particles.

In order to magnetize the pads in a controlled direction, an external magnet was placed close to the device with magnetic field aligned in the direction of the bar's long axis, using shape anisotropy to induce constant magnetization in the bar¹⁹. To validate the direction of the magnetic field the substrate was imaged under a magneto-optic microscope, confirming the edges as magnetic poles (see Fig. S1).

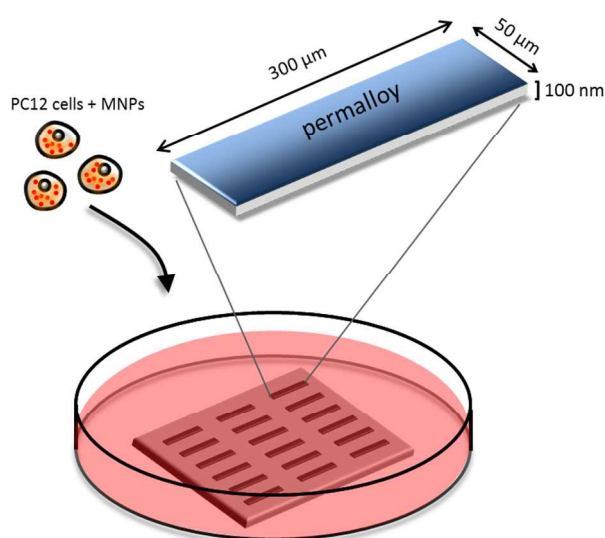


Fig. 3 An illustration describing the size of the permalloy patterns.

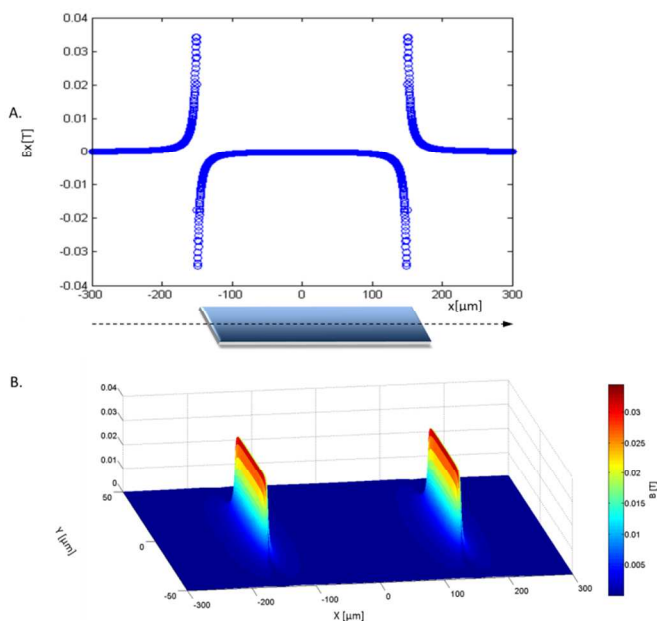


Fig. 4 The magnetic flux density (B_x) as simulated in MATLAB at $1 \mu\text{m}$ above a ferromagnetic line, presented in 2D (A) and 3D (B).

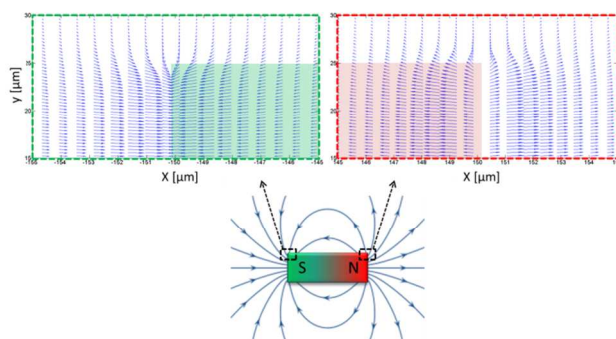


Fig. 5 The direction of the magnetic field at $1 \mu\text{m}$ above the edges of a ferromagnetic line, as simulated in MATLAB.

Organizing PC12 cells atop the magnets embedded device

To study the effect of the micro-magnetic device on cells motility, PC12 cells in suspension were incubated with MNPs (as described in the experimental section) and plated atop the device. Fig. 6(A) (left panel) presents the distribution of cells atop the magnetic lines immediately after plating. It can be seen that there is no correlation between the cells' locations and the lines, cells are spread homogeneously atop the device. Five days later, the PC12 cells with the MNPs settled down atop the micropatterned magnetic device, as shown in Fig. 6(A) (middle panel). Now the cells display a non-homogeneous distribution with a preference to the magnetic bars and specifically to the edges. This corroborates that the cells with MNPs are indeed affected by the micro-magnets and attracted to the magnetic 'hot spots' at the bar' poles. Fig. 6(A) (right panel) presents the same device with cultured PC12 cells with no MNPs, at the same age as the affected cells (middle). It can be seen that with no MNPs there is no correlation between the magnetic bars and cells' location. Since the magnetic bars are opaque, we could not optically image the cells above them. To analyze the distribution of PC12 cells atop the lines the cells that contained fluorescent MNPs were imaged fluorescently. Fig. 6(B) (left) demonstrates the attraction of the magnetized cells to the tips of the lines. The average fluorescence intensity along the long axis of the magnetic bars is presented in Fig. 6(B) (right). Higher levels of fluorescence can be detected close to the edges.

Experimental

Magnetic simulations and calculations

Magnetic simulations were performed by using the OOMMF micromagnetic simulation software (ITL/NIST), in order to find the remanence magnetization of the ferromagnets. The software integrates the Landau–Lifshitz equation on a 2D grid with 3D magnetization spins. The magnetic field created by the magnetic dipole of the ferromagnet²⁰ was numerically calculated using a MATLAB script, taking into account the size of the ferromagnets and the material they are made of. All components of the magnetic field along a ferromagnet were calculated at $1 \mu\text{m}$ above the ferromagnet.

ARTICLE

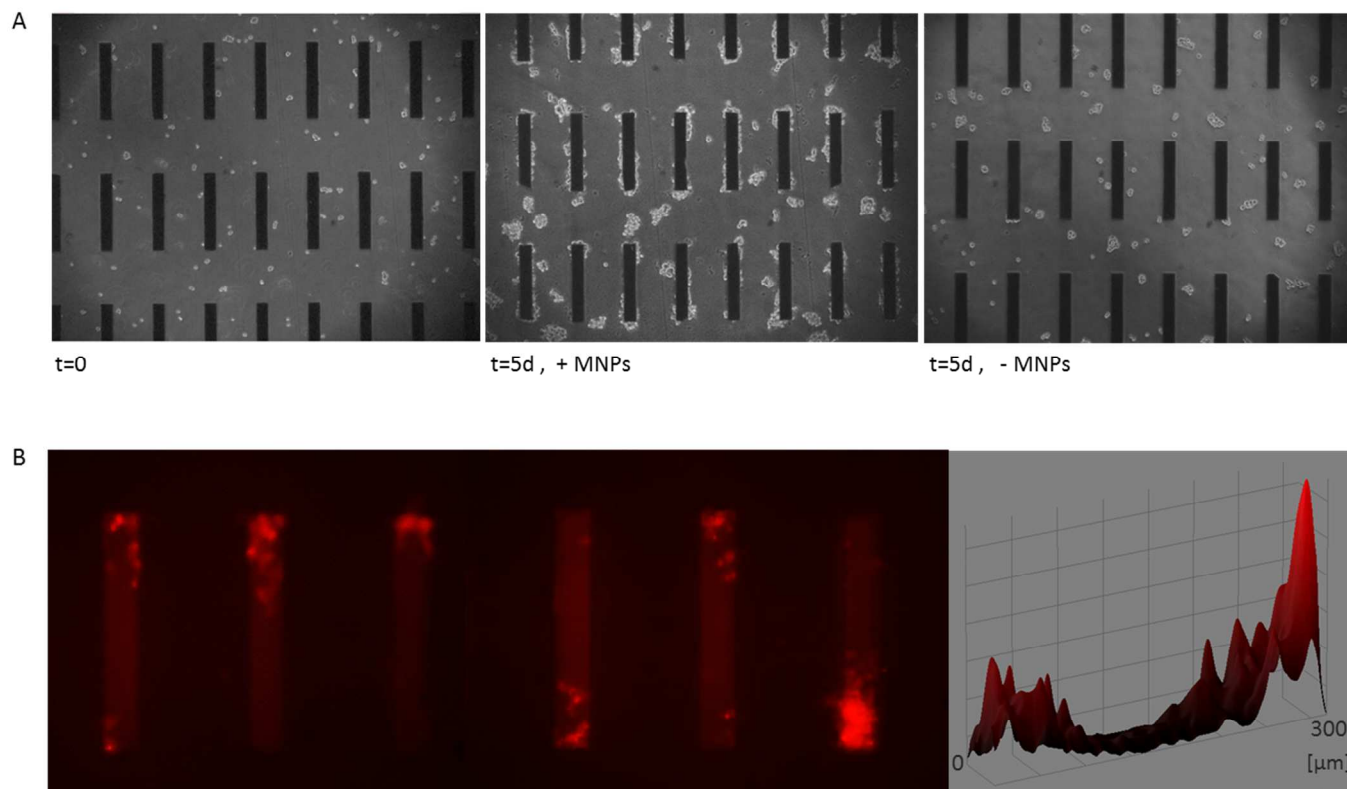


Fig. 6 PC12 cells with MNPs atop the magnetic patterns. (A) Phase contrast images of the cells interact with the ferromagnets at $t=0$ (left), after 5 days with the treatment of MNPs (middle), and after 5 days without the treatment of MNPs (right). (B) A fluorescent image of cells treated with the fluorescent MNPs on the magnetic bars 5 days after plating (left). The average of the fluorescence intensity along the magnetic bars (right).

Fabrication of ferromagnetic patterned substrates

The ferromagnetic patterns consisted of rectangles made of permalloy in the size of $300 \times 50 \mu\text{m}^2$, with lateral spacing of $150 \mu\text{m}$ and vertical spacing of $200 \mu\text{m}$ (Fig. 4). The patterns were fabricated by a standard photolithography method, as previously described by Baranes et al.²¹, with few modifications. Briefly, the glass substrates were ultrasonically cleaned using acetone/ ethanol/ isopropanol, and dried by high purity nitrogen. S1813 resist (Shipley Company LLC, Marlborough, MA, USA) was spin coated on the glass substrate and then baked at 115°C . Next, the patterns were transferred to the resist and developed in MF-319 (Rohm and Haas, Philadelphia, PA, USA). The samples were transferred to the deposition chamber and were cleaned in Ar plasma prior to deposition. We deposit a 3 nm Al adhesion layer followed by a 74 nm permalloy layer and a 3 nm of Nb layer. Finally, the non-patterned photoresist is removed by soaking the sample in acetone for an hour.

Synthesis of magnetic nanoparticles containing the fluorescent probe rhodamine

Maghemite MNPs labelled with the fluorescent probe rhodamine ($R\text{-}\gamma\text{-Fe}_2\text{O}_3$) were synthesized and characterized according to a previously described method²², which was modified to the specifications and requirements of our magnetic device. Briefly, rhodamine isothiocyanate (RITC) was covalently conjugated to gelatin by adding 0.5 ml DMSO containing 5 mg RITC to 20 ml aqueous solution containing 1% w/v gelatin. The pH of the aqueous solution was then raised to 9.5 by adding NaOH aqueous solution (1 M). Then, the solution was shaken for 1 h at 60°C . The RITC conjugated gelatin solution was then dialyzed at 60°C against water to remove excess of unbound RITC. The volume of the solution was then adjusted to 80 ml by adding water. Then, $160 \mu\text{l}$ of Fe^{2+} solution (10 mmol in 5 ml of 0.1 M HCl) and $57.6 \mu\text{l}$ of sodium nitrite solution (7.27 mmol in 5 ml H_2O) were added to the shaken gelatin solution. For nucleation, titration with NaOH (1 M) until pH of 9.5 was performed. This procedure was repeated six more times to achieve stronger magnetization of the particles. The reaction mixture was then shaken at 60°C for an additional 1 h. The formed $R\text{-}\gamma\text{-Fe}_2\text{O}_3$ MNPs were then washed from non-magnetic waste with deionized water by the high gradient magnetic field (HGFMF) technique. The final concentration of the particles was 9 mg/ml. The size of the

MNPs was measured using TEM, presenting a dry diameter of 15.0 ± 1.4 nm. The hydrodynamic diameter of the particles dispersed in aqueous continuous phase, as determined by the light scattering technique, was 120 ± 12 nm.

Magnetic field measurements

A digital gaussmeter (Scientific Equipment Roorkee, DGM-204) was used to measure the magnetic field induced by the external permanent magnet.

Cell culture

Rat pheochromocytoma PC12 cells (ATCC) were cultured in suspension in RPMI medium supplemented with 10% horse serum, 5% fetal bovine serum, 1% penicillin-streptomycin, 1% L-glutamine and 0.2% amphotericin. The cells were cultured in 75 cm² flasks and maintained at 37 °C in a humidified incubator containing 5% CO₂. For the magnetic patterning experiments, the cells were incubated with 600 µg/ml of MNPs in complete medium at 37 °C for 24 h, to allow the particles to interact with the cells. The cells were then washed twice and plated in a 35 mm culture dish containing a ferromagnetic patterned substrate.

Cell viability

The viability of the cells was assessed using a colorimetric XTT assay. The assay is based on the ability of metabolic active cells to reduce tetrazolium salt XTT to orange colored compounds of formazan. The intensity of the dye is proportional to the number of metabolic active cells. 10⁴ PC12 cells were seeded on 96-well plates, in the absence and presence of MNPs. After 24 hours or 72 hours of MNPs exposure, XTT reaction solution (Biological Industries, Israel) was added to the medium and incubated for 5 hours at 37°C. Absorbance was measured using a spectrophotometer (BioTek Synergy4, Vermont USA) at 450nm and 630nm as background.

Imaging

Time-lapse live microscopy. Images were taken by a CCD camera (Q Imaging Retiga 2000R) mounted on a phase contrast microscope (Nikon Eclipse TE2000-E), enclosed in a temperature, CO₂ and humidity controlled chamber (magnification X40, NA=0.6).

Fluorescence microscopy. Fluorescent images of the cells atop the ferromagnetic device were taken by Leica DFC 360 FX camera mounted on a Leica Z16 APO upright stereomicroscope (magnification 45X, NA=0.5). Confocal imaging of the cells in high magnification was performed using a Leica TCS SP5 microscope with an Acousto-Optical Beam Splitter. (magnification X63, NA=1.2)

Magneto-optic Faraday imaging. We measure the out-of-plane component of the local magnetic field via the Faraday effect and a magneto-optically sensitive thin yttrium iron garnet (YIG) plate that was placed on the magnetic device. The full setup is shown in reference²⁵. A constant bar magnet was used to align the magnetic bars to the elongated direction of the bar in the sample plane.

Image analysis

Histograms of the intensity of fluorescence, indicating the accumulation of cells along the ferromagnets, was created using ImageJ software.

Conclusions

This study demonstrates the application of controllable magnetic fields on PC12 cells labelled with fluorescent MNPs in order to direct cell migration and growth. Applying an external magnetic field has led to a directed movement of PC12 cells. Furthermore, we have designed and fabricated a ferromagnetic micropatterned device that induces highly localized magnetic fields and could be uniquely controlled due to its geometry and material properties. The magnetic device enabled us to position PC12 cells in a desired pattern according to the magnetic flux generated by the micro ferromagnets. Previously an array of deposited magnetic patterns has been used in the presence of an external magnetic field to manipulate magnetic particles within cells^{18,26,27}. Here we were able to manipulate the cells without applying an additional external magnetic field. Our results suggest the micropatterned magnetic device as a platform for guiding populations of cells in a pre-programmed controllable manner. The miniaturization of the common used permanent magnets to an array of magnetic pads in a microscopic resolution sets the stage for the design of implanted devices for therapeutic applications and for the potential design of bioelectronics.

Acknowledgements

We thank Dr. Avraham Chelly for his assistance with the magnetic measurements, and Daniel Levi for his help in the magneto-optics microscopy. We thank Keren Hasidim and Michal Yossef that contributed to the first stages of simulation work.

Notes and references

a Faculty of Engineering, Bar Ilan University, Ramat Gan, 5290002, Israel.

b Physics department, Bar Ilan University, Ramat Gan, 5290002, Israel.

c Chemistry department, Bar Ilan University, Ramat Gan, 5290002, Israel.

d Institute of Nanotechnologies and Advanced Materials, Bar Ilan University, Ramat Gan, 5290002, Israel.

† Corresponding authors: Orit Shefi (orit.shefi@biu.ac.il) and Amos Sharoni (amos.sharoni@biu.ac.il)

Electronic Supplementary Information (ESI) available: For a figure of a magneto-optics imaging of ferromagnetic bars (Fig. S1) and the calculations of number of MNPs per cell See DOI: 10.1039/b000000x/

1 D. Bray, *J. Cell Sci.*, 1979, **37**, 391–410.

2 D. Bray, *Dev. Biol.*, 1984, **102**, 379–89.

3 J. Zheng, P. Lamoureux, V. Santiago, T. Dennerll, R. E. Buxbaum and S. R. Heidemann, *J. Neurosci.*, 1991, **11**, 1117–1125.

4 K. Franze and J. Guck, *Rep. Prog. Phys.*, 2010, **73**, 094601.

5 A. Ayali, *Integr. Biol. Quant. Biosci. Nano Macro*, 2010, **2**, 178–182.

6 P. Lamoureux, R. E. Buxbaum and S. R. Heidemann, *Nature*, 1989, **340**, 159–162.

7 P. Lamoureux, G. Ruthel, R. E. Buxbaum and S. R. Heidemann, *J. Cell Biol.*, 2002, **159**, 499–508.

8 J. N. Fass and D. J. Odde, *Biophys. J.*, 2003, **85**, 623–636.

Journal Name

- 9 T. M. Fischer, P. N. Steinmetz and D. J. Odde, *Ann. Biomed. Eng.*, 2005, **33**, 1229–1237.
- 10 C. F. Blackman, S. G. Benane and D. E. House, *FASEB J. Off. Publ. Fed. Am. Soc. Exp. Biol.*, 1993, **7**, 801–6.
- 11 G. Ciofani, V. Raffa, A. Menciassi, A. Cuschieri and S. Micera, *Biomed. Microdevices*, 2009, **11**, 517–27.
- 12 C. Riggio, M. P. Calatayud, C. Hoskins, J. Pinkernelle, B. Sanz, T. E. Torres, M. R. Ibarra, L. Wang, G. Keilhoff, G. F. Goya, V. Raffa and A. Cuschieri, *Int. J. Nanomedicine*, 2012, **7**, 3155–3166.
- 13 J. A. Kim, N. Lee, B. H. Kim, W. J. Rhee, S. Yoon, T. Hyeon and T. H. Park, *Biomaterials*, 2011, **32**, 2871–2877.
- 14 M. Marcus, H. Skaat, N. Alon, S. Margel and O. Shefi, *Nanoscale*, 2014.
- 15 C. Riggio, M. P. Calatayud, M. Giannaccini, B. Sanz, T. E. Torres, R. Fernández-Pacheco, A. Ripoli, M. R. Ibarra, L. Dente, A. Cuschieri, G. F. Goya and V. Raffa, *Nanomedicine Nanotechnol. Biol. Med.*, 2014.
- 16 H. Lee, A. M. Purdon and R. M. Westervelt, *IEEE Trans. Magn.*, 2004, **40**, 2991–2993.
- 17 H. Lee, A. M. Purdon and R. M. Westervelt, *Appl. Phys. Lett.*, 2004, **85**, 1063.
- 18 P. Tseng, D. Di Carlo and J. W. Judy, *Nano Lett.*, 2009, **9**, 3053–3059.
- 19 J. M. D. Coey, *Magnetism and Magnetic Materials*, Cambridge University Press, 2010.
- 20 W. J. Duffin, *Electricity and Magnetism*, Mc, Fourth.
- 21 K. Baranes, N. Chejanovsky, N. Alon, A. Sharoni and O. Shefi, *Biotechnol. Bioeng.*, 2012, **109**, 1791–1797.
- 22 H. Skaat, G. Belfort and S. Margel, *Nanotechnology*, 2009, **20**, 225106.
- 23 H. Skaat, O. Ziv-Polat, A. Shahar and S. Margel, *Bioconjug. Chem.*, 2011, **22**, 2600–2610.
- 24 K. Baranes, D. Kollmar, N. Chejanovsky, A. Sharoni and O. Shefi, *J. Mol. Histol.*, 2012, **43**, 437–447.
- 25 M. Baziljevich, D. Barness, M. Sinvani, E. Perel, A. Shaulov and Y. Yeshurun, *Rev. Sci. Instrum.*, 2012, **83**, 083707.
- 26 P. Tseng, J. W. Judy and D. Di Carlo, *Nat. Methods*, 2012, **9**, 1113–1119.
- 27 P. Tseng and D. Di Carlo, *Methods Cell Biol.*, 2014, **120**, 201–214.